J|A|C|S
ARTICLES
Published on Web 12/05/2006

Planar Trimethylenemethane Dianion Chemistry of Lanthanide Metallocenes: Synthesis, Structure, Density Functional Theory Analysis, and Reactivity of $[(C_5Me_5)_2Ln]_2[\mu\text{-}\eta^3\text{:}\eta^3\text{-}C(CH_2)_3]$ Complexes

William J. Evans,*,† Timothy M. Champagne,† Joseph W. Ziller,† and Nikolas Kaltsoyannis*,‡

Contribution from the Department of Chemistry, University of California, Irvine, California 92697-2025, and Department of Chemistry, University College London, 20 Gordon Street, London WC1H 0AJ, United Kingdom

Received June 28, 2006; E-mail: wevans@uci.edu; n.kaltsoyannis@ucl.ac.uk

Abstract: The unusual formation of planar trimethylenemethane (TMM) dianion complexes of lanthanide metallocenes, $[(C_5Me_5)_2Ln]_2[\mu\text{-}\eta^3\text{:}\eta^3\text{-}C(CH_2)_3]$ (Ln = Sm, **1**; La, **2**; Pr, **3**; Nd, **4**; Y, **5**) has been examined by synthesizing examples with metals from La to Y to examine the effects of radial size on structure and to provide closed shell examples for direct comparison with density functional theory (DFT) calculations. Synthetic routes to **1**−**4** have been expanded from the $[(C_5Me_5)_2Ln][(\mu\text{-}Ph)_2BPh_2]$/neopentyl lithium reaction involving β-methyl elimination to a $[(C_5Me_5)_2Ln][(\mu\text{-}Ph)_2BPh_2]$/isobutyl lithium route. The synthetic pathways are sensitive to metal radius. To obtain **5**, the methylallyl complex, $(C_5Me_5)_2Y[CH_2C(Me)CH_2]$, **6**, was synthesized and treated with $[(C_5Me_5)_2YH]_x$. In the Lu case, the neopentyl complex $[(C_5Me_5)_2LuCH_2C(CH_3)_3]_x$, **7**, was isolated instead of the TMM product. X-ray crystallography showed that the metrical parameters of the planar TMM dianions in each complex are similar. The structural data have been compared with DFT calculations on the closed-shell lanthanum and lutetium complexes that suggest only limited covalent interactions with the lanthanide ion. Benzophenone (2 equiv) reacts with **1** to expand the original four-carbon TMM skeleton to a dianionic bis(alkoxide) ligand containing a symmetrically substituted $C{=}CH_2$ moiety in $[(C_5Me_5)_2Sm]_2[\mu\text{-}(OCPh_2CH_2)_2C{=}CH_2]$, **8**. In this reaction, the TMM complex reacts as a bifunctional bisallylic reagent that generates an organic framework containing a central vinyl group.

Introduction

Recent studies of the reaction chemistry of the metallocene cations, $[(C_5Me_5)_2Ln][(\mu\text{-}Ph)_2BPh_2]$, with alkyl lithium reagents have shown that this reaction is an excellent route to unsolvated $[(C_5Me_5)_2LnR]_n$ complexes, eq 1.[1,2] When the reaction of

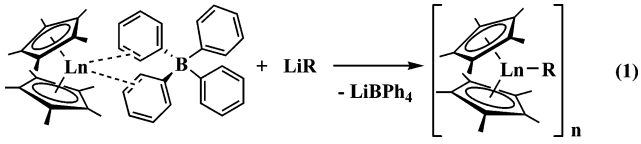

(1)

neopentyl lithium with the samarium cation was examined, the product was surprisingly found to have four carbon atoms instead of the five carbons in the organolithium precursor and was identified as a trimethylenemethane (TMM) complex, $[(C_5Me_5)_2Sm]_2[\mu\text{-}\eta^3\text{:}\eta^3\text{-}C(CH_2)_3]$, **1**, eq 2, Figure 1. Subsequent modeling of the intermediate reactions leading to the TMM product suggested that β-alkyl elimination followed by metalation was occurring as shown in Scheme 1.[2]

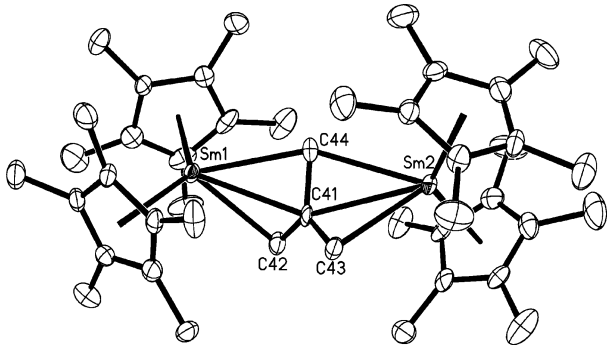

Figure 1. Thermal ellipsoid plot of $[(C_5Me_5)_2Sm]_2[\mu\text{-}\eta^3\text{:}\eta^3\text{-}C(CH_2)_3]$, **1**, with the probability ellipsoids drawn at the 50% level. Hydrogen atoms have been excluded for clarity.

Although several examples of TMM complexes have been reported in the literature,[2−7] the TMM ligand in **1** was the first

† University of California, Irvine.
‡ University College London.

(1) Evans, W. J.; Perotti, J. M.; Ziller, J. W. *J. Am. Chem. Soc.* **2005**, *127*, 3894.
(2) Evans, W. J.; Perotti, J. M.; Ziller, J. W. *J. Am. Chem. Soc.* **2005**, *127*, 1068.
(3) Kissounko, D. A.; Sita, L. R. *J. Am. Chem. Soc.* **2004**, *126*, 5946.
(4) Herberich, G. E.; Kreuder, C.; Englert, U. *Angew. Chem., Int. Ed. Engl.* **1994**, *33*, 2465.
(5) Mayer, J. M.; Curtis, C. J.; Bercaw, J. E. *J. Am. Chem. Soc.* **1983**, *105*, 2651.
(6) Keaton, R. J.; Sita, L. R. *Organometallics* **2002**, *21*, 4315.
(7) Gobbi, A.; MacDougall, P. J.; Frenking, G. *Angew. Chem., Int. Ed. Engl.* **1991**, *30*, 1001.

10.1021/ja0645988 CCC: $33.50

Scheme 1

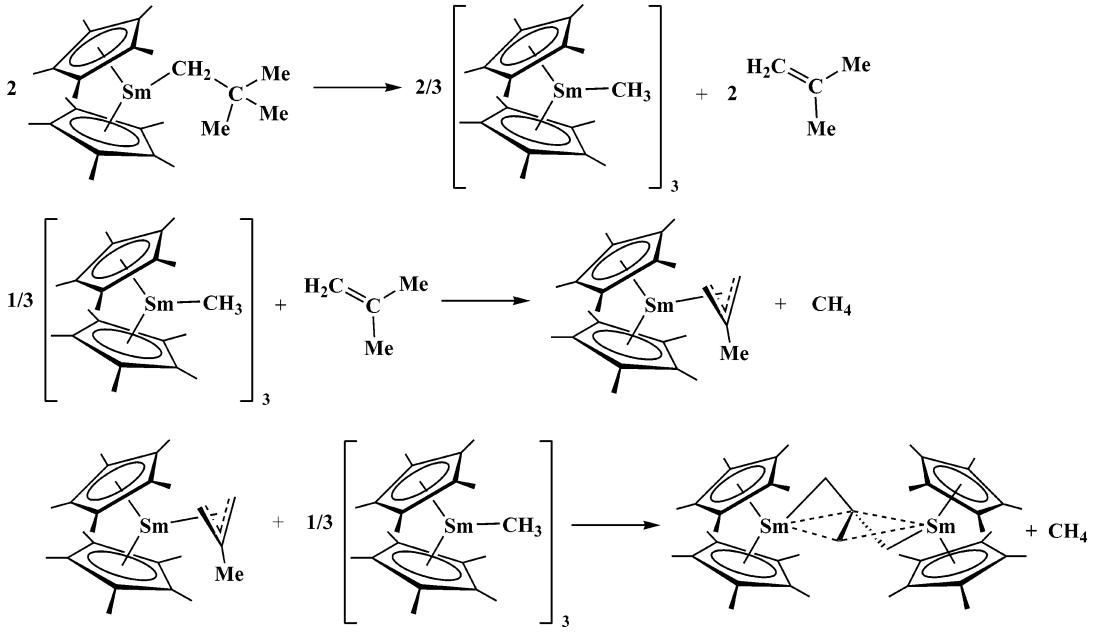

example of both a planar and bridging TMM. Due to the unique nature of this unit, efforts to analyze its bonding with samarium were pursued using density functional theory. As described here, these were unsuccessful with this $4f^5$ system. However, as

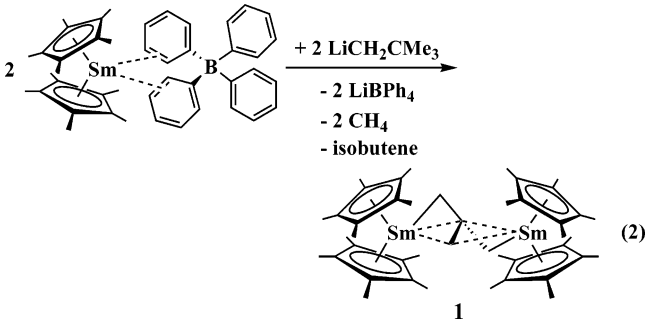

described in more detail below, calculations on the diamagnetic lanthanum analogue, $[(C_5Me_5)_2La]_2[\mu\text{-}\eta^3\text{:}\eta^3\text{-}C(CH_2)_3]$, **2**, did converge. Surprisingly, the geometry obtained computationally for **2** did not agree with the original X-ray crystal structure of **1**, which was of low quality. However, a higher quality structure of **1** was subsequently obtained and found to be in agreement with the calculations.

To obtain crystallographic data on the lanthanum complex, **2**, for direct comparison with the calculation and with the structure of **1**, the reaction chemistry of the lanthanum cation, $[(C_5Me_5)_2La][(\mu\text{-}Ph)_2BPh_2]$, with neopentyl lithium was examined. $[(C_5Me_5)_2La]_2[\mu\text{-}\eta^3\text{:}\eta^3\text{-}C(CH_2)_3]$, **2**, was isolated and fully characterized by X-ray crystallography, and the structural results are compared here with density functional theory analysis. X-ray crystallographic data were also obtained on the Pr, **3**, Nd, **4**, and Y, **5**, analogues to examine structural changes in TMM binding as a function of the size and electronic configuration of the metal.

Since the pathway to the TMM complex **1** involved metalation of isobutene, it was conceivable that these TMM complexes could also be accessed from the reactions of the $[(C_5Me_5)_2Ln][(\mu\text{-}Ph)_2BPh_2]$ cations with isobutyl lithium rather than neopentyl lithium. This sequence has been examined with the two diamagnetic lanthanide metals, La and Lu, as well as the diamagnetic congener Y.

We also present the first reactivity studies of these f element TMM complexes and show that they readily react as bifunctional organometallics containing a central vinyl moiety. Hence, two equiv of benzophenone react with the four-carbon TMM ligand to make a six-carbon unit with two terminal oxygen functionalities and a central vinyl component.

Experimental Section

The manipulations described below were performed under argon with rigorous exclusion of air, water, and coordinating solvents using Schlenk, vacuum line, and glovebox techniques. 1-Chloro-2-methylpropane (isobutyl chloride) and 1-chloro-2,2-dimethylpropane (neopentyl chloride) were purchased from Aldrich and distilled onto activated 4 Å molecular sieves under argon. $[(C_5Me_5)_2Sm]_2[\mu\text{-}\eta^3\text{:}\eta^3\text{-}C(CH_2)_3]$,[2] **1**, $[(C_5Me_5)_2Ln][(\mu\text{-}Ph)_2BPh_2]$ (Ln = La,[8] Pr,[9] Nd,[10] Sm,[10] and Lu[1]), and $[(C_5Me_5)_2YH]_x$[10] were prepared as previously reported. $(C_5Me_5)_2Y(\mu\text{-}Cl)K(THF)_2$ was synthesized from $LnCl_3$ and KC_5Me_5 according to literature methods.[11] Isobutyl lithium and neopentyl lithium were prepared by adding isobutyl chloride and neopentyl chloride, respectively, to excess lithium granules (Strem) in hexane (150 mL) and heating at reflux for 1 week.[12] 2-Methylpropene (Matheson) and 2-methylpropene-d_8 (Aldrich) were used as received. Solvents were sparged with UHP argon (Airgas) and dried over columns containing Q-5 and sieves. NMR solvents (Cambridge Isotopes) were dried over benzophenone-ketyl, degassed, and vacuum transferred before use. ^1H and ^{13}C NMR spectra were recorded with Bruker DRX 400 and 500 MHz spectrometers. Infrared spectra were recorded as thin films on an

(8) Evans, W. J.; Davis, B. L.; Ziller, J. W. *Inorg. Chem.* **2001**, *40*, 6341.
(9) Evans, W. J.; Perotti, J. M.; Kozimor, S. A.; Champagne, T. M.; Davis, B. L.; Nyce, G. W.; Fujimoto, C. H.; Clark, R. D.; Johnston, M. A.; Ziller, J. W. *Organometallics* **2005**, *24*, 3916.
(10) Evans, W. J.; Seibel, C. A.; Ziller, J. W. *J. Am. Chem. Soc.* **1998**, *120*, 6745.
(11) Evans, W. J.; Keyer, R. A.; Ziller, J. W. *Organometallics* **1993**, *12*, 2618.
(12) Schlosser, M. *Organometallics in Synthesis: A Manual*; John Wiley and Sons Ltd.: 2001.

ASI ReactIR 1000 spectrometer.[13] Elemental analyses were performed by Analytische Laboratorien (Lindlar, Germany) and complexometric titration.[14]

[(C5Me5)2Sm]2[μ-η3:η3-C(CH2)3], 1. Isobutyl lithium (7 mg, 0.11 mmol) in 5 mL of methylcyclohexane was added dropwise to a stirred solution of freshly recrystallized [(C5Me5)2Sm][(μ-Ph)2BPh2] (80 mg, 0.11 mmol) in 10 mL of methylcyclohexane. The red mixture immediately became cloudy and after 4 h turned orange. Insoluble material was removed by centrifugation, and removal of solvent yielded **1** as a glassy orange-brown solid (27 mg, 28%). NMR analysis of **1** matched the previously reported complex.[2] Isobutane was observed by ^{1}H NMR spectroscopy at δ 0.91 (d, 9H, (CH_3)$_3$CH), 1.96 (m, 1H, (CH$_3$)$_3$CH), and analysis of the insoluble material revealed the presence of [(C5Me5)2Sm(μ-H)]2.[15]

[(C5Me5)2La]2[μ-η3:η3-C(CH2)3], 2. Neopentyl lithium (8 mg, 0.10 mmol) in 5 mL of methylcyclohexane was added dropwise to a stirred solution of freshly recrystallized [(C5Me5)2La][(μ-Ph)2BPh2] (71 mg, 0.10 mmol) in 10 mL of methylcyclohexane. The clear mixture immediately became cloudy and after 4 h turned green. Insoluble material was removed by centrifugation, and removal of solvent yielded **2** as a green tacky solid (60 mg, 70%). Yellow-green crystals of **2** suitable for X-ray diffraction were grown by slow evaporation of a methylcyclohexane solution at 25 °C. Anal. Calcd for $C_{44}H_{66}La_2$: C, 61.93; H, 7.64; La, 31.82. Found: C, 62.51; H, 7.60; La, 31.10. ^{1}H NMR (C_6D_{12}, 25 °C) δ 1.97 (s, 6H, C(CH_2)$_3$), 1.96 (s, 60H, C$_5$$Me_5$). ^{13}C NMR δ 10.49 (C$_5$$Me_5$), 64.23 (C(C$H_2$)$_3$), 118.68 (C$_5Me_5$). IR (thin film) 2961s, 2926s, 2876s, 2729w, 1567w, 1517w, 1459m, 1378w, 1247w, 1065w, 726w cm^{-1}.

Compound 2 from [(C5Me5)2La][(μ-Ph)2BPh2] and ^{i}BuLi. As described above, isobutyl lithium (4 mg, 0.06 mmol) in 5 mL of methylcyclohexane was added to freshly crystallized [(C5Me5)2La][(μ-Ph)2BPh2] (43 mg, 0.06 mmol) in 10 mL of methylcyclohexane. The pale yellow mixture immediately became cloudy and after 4 h turned yellow-green. Insoluble material was removed by centrifugation, and removal of solvent yielded **2** as a green tacky solid (7 mg, 14%).

[(C5Me5)2Pr]2[μ-η3:η3-C(CH2)3], 3. As described above, neopentyl lithium (5 mg, 0.06 mmol) in 5 mL of methylcyclohexane was added to freshly crystallized [(C5Me5)2Pr][(μ-Ph)2BPh2] (42 mg, 0.06 mmol) in 10 mL of methylcyclohexane to yield a yellow tacky solid (32 mg, 62%). Yellow crystals of **3** suitable for X-ray diffraction were grown from a concentrated methylcyclohexane solution at −36 °C. Anal. Calcd for $C_{44}H_{66}Pr_2$: Pr, 32.1. Found: Pr, 32.4. ^{1}H NMR (C_6D_{12}, 25 °C) δ 3.15 (br s, 6H, C(CH_2)$_3$), 2.41 (br s, 60H, C$_5$$Me_5$). ^{13}C NMR δ −2.73 (C$_5$$Me_5$), −12.87 (C(C$H_2$)$_3$). IR (thin film) 2961s, 2926s, 2876s, 2729w, 1532w, 1463m, 1378w, 1243w, 1065w, 1038w, 726w cm^{-1}.

[(C5Me5)2Nd]2[μ-η3:η3-C(CH2)3], 4. As described above, neopentyl lithium (8 mg, 0.10 mmol) in 5 mL of methylcyclohexane was added dropwise to freshly recrystallized [(C5Me5)2Nd][(μ-Ph)2BPh2] (69 mg, 0.09 mmol) in 10 mL of methylcyclohexane to yield a green tacky solid (49 mg, 59%). Green crystals of **4** suitable for X-ray diffraction were grown from a concentrated methylcyclohexane solution at −36 °C. Anal. Calcd for $C_{44}H_{66}Nd_2$: Nd, 32.6. Found: Nd, 32.1. ^{1}H NMR (C_6D_{12}, 25 °C) δ 6.49 (br s, 6H, C(CH_2)$_3$), 5.25 (br s, 60H, C$_5$$Me_5$). ^{13}C NMR δ −18.23 (C$_5$$Me_5$), −18.78 (C(C$H_2$)$_3$). IR (thin film) 2961s, 2926s, 2876s, 2729w, 1532w, 1459m, 1378w, 1247w, 1065w, 1038w, 722w cm^{-1}.

(C5Me5)2Y[CH2C(Me)CH2], 6. [CH$_2$C(Me)CH$_2$]MgCl (4.62 mL, 2.31 mmol) was added dropwise via syringe to a stirred slurry of (C$_5$Me$_5$)$_2$YCl$_2$K(THF)$_2$ (1.41 g, 2.30 mmol) in 100 mL of toluene. The mixture eventually changed color to form a yellow slurry. After 1 day, insoluble material was removed from the pale yellow mixture by centrifugation and filtration. The solvent was removed leaving a yellow oil. The oil was extracted with 100 mL of a dioxane/hexane solution (1:10) and stirred. After 12 h, insoluble material was removed from the pale yellow mixture by centrifugation and filtration. The solvent was removed leaving a yellow oily solid. The solid was redissolved in 20 mL of toluene, and volatiles were subsequently removed under a vacuum. The resulting yellow oil was dissolved in 20 mL of hexane, and volatiles were subsequently removed leaving **6** as a yellow powdery solid (0.98 g, 87%). Anal. Calcd for $C_{44}H_{66}Y_2$: C, 70.05; H, 8.35; Y, 21.61. Found: C, 69.86; H, 8.52; Y, 21.50. ^{1}H NMR (C_6D_6, 25 °C) δ 1.96 (s, 33H, C$_5$$Me_5$, CH$_2$C(C$H_3$)CH$_2$), 2.18 (s, 4H, 2.5 Hz, CH_2C(CH$_3$)CH_2). ^{13}C NMR δ 11.65 (C$_5$$Me_5$), 29.46 (CH$_2$C(C$H_3$)CH$_2$), 64.70 (d, 2.25 Hz, C$H_2$C(CH$_3$)C$H_2$), 117.81 (C$_5Me_5$), 170.48 (CH$_2$C(CH$_3$)CH$_2$).

[(C5Me5)2Y]2[μ-η3:η3-C(CH2)3], 5. Complex **6** (47 mg, 0.11 mmol) was added slowly to a slurry of freshly prepared [(C5Me5)2YH]$_x$ (42 mg, 0.12 mmol) in 10 mL of methylcyclohexane. The white mixture immediately changed color to form a yellow mixture. The mixture was filtered to remove insoluble material, and removal of solvent left **5** as a bright yellow solid (66 mg, 75%). Anal. Calcd for $C_{44}H_{66}Y_2$: C, 68.37; H, 8.62; Y, 23.00. Found: C, 68.06; H, 8.81; Y, 23.35. ^{1}H NMR (C_6D_{12}, 25 °C) δ 1.98 (s, 6H, C(CH_2)$_3$), 1.96 (s, 60H, C$_5$$Me_5$). ^{13}C NMR δ 11.85 (C$_5$$Me_5$), 52.10 (C(C$H_2$)$_3$), 118.10 (C$_5Me_5$), 175.72 (C(CH$_2$)$_3$). IR (thin film) 2961s, 2926s, 2876s, 2729w, 1567w, 1517w, 1459m, 1378w, 1247w, 1065w, 726w cm^{-1}. Yellow crystals of **5** suitable for X-ray diffraction were initially grown from a C_6D_{12} solution in an NMR tube at 25 °C from the following mixed metal reaction. (C$_5$Me$_5$)$_2$Y[CH$_2$C(Me)CH$_2$] (17 mg, 0.04 mmol) was added slowly to a slurry of freshly prepared [(C5Me5)2LuH]$_x$ (18 mg, 0.04 mmol) in 2 mL of C_6D_{12}. The white mixture immediately changed color to form a yellow mixture upon addition. The mixture was filtered to remove insoluble material leaving a clear yellow solution which was transferred to an NMR tube.

(C5Me5)2Lu(CH2CMe3), 7. A solution of neopentyl lithium (7 mg, 0.09 mmol) in 5 mL of methylcyclohexane was added dropwise to a stirred solution of [(C5Me5)2Lu][(μ-Ph)2BPh2] (61 mg, 0.08 mmol) in 10 mL of methylcyclohexane. The clear mixture immediately became cloudy and eventually became yellow. After 5 h, insoluble material was removed by centrifugation, and removal of solvent yielded **6** as a yellow solid (Yield 35 mg, 86%). Anal. Calcd for $C_{25}H_{41}Lu$: C, 58.12; H, 8.02; Lu, 33.87. Found: C, 57.92; H, 7.88; Lu, 34.20. ^{1}H NMR (C_6D_{12}, 25 °C) δ 1.96 (s, 30H, C$_5$$Me_5$), 0.99 (s, 9H, CH$_2CMe_3$), 0.23 (s, 2H, C$H_2CMe_3$). ^{13}C NMR δ 10.9 (C$_5$$Me_5$), 29.4 (C$Me_3$), 49.1 (C$H_2$), 118.4 (C$_5Me_5$). The quaternary carbon could not be located. IR (thin film) 2922s, 2853s, 2795w, 2663w, 1567w, 1447m, 1374w, 1347w, 1305w, 1262w, 1092w, 1031w, 965m cm^{-1}.

[(C5Me5)2Sm]2[μ-(OCPh2CH2)2C=CH2)], **8**. A solution of **1** (95 mg, 0.106 mmol) in 5 mL of hexane was added dropwise to a stirred solution of freshly sublimed benzophenone (19 mg, 0.106 mmol) in 10 mL of hexane. After 1 h, the deep yellow solution was filtered, and removal of solvent yielded **5** as a yellow solid (85 mg, 64%). Yellow crystals of **5** suitable for X-ray diffraction were grown from a concentrated hexane solution at −36 °C. Anal. Calcd for $C_{58}H_{106}O_2Sm_2$: Sm, 23.9. Found: Sm, 23.5. ^{1}H NMR (C_6D_6, 25 °C) δ 0.72 (s, 60H, C$_5$$Me_5$), 2.49 (s, 4H, CH$_2$C(C$H_2$)$_2$), 5.35 (s, 2H, CH$_2$C(C$H_2$)$_2$), 7.02, 7.23, 8.05 (m, 20H, C$_6$$H_5$). ^{13}C NMR δ 17.63 (C$_5$$Me_5$), 118.49 (C$_5Me_5$), 2.49 (CH$_2$C(CH$_2$)$_2$), 5.35 (CH$_2$C(CH$_2$)$_2$), 7.02, 7.23, 8.05 (m, 20H, C$_6$H$_5$). IR (thin film) 3057m, 3022m, 2960s, 2906s, 2856s, 1617s, 1571m, 1490m, 1447m, 1327s, 1289s, 1181m, 1061s, 1026m, 1003m, 768w, 702w cm^{-1}.

(C5Me5)2La(CH2Ph), 9. Toluene (1 mL) was added directly onto a stirred solution of **2** (23 mg, 0.026 mmol) in 5 mL of methylcyclohexane. The green solution immediately became reddish-brown. After 1 h, evaporation of solvent yielded a brown oily solid (12 mg, 89%). Anal. Calcd for $C_{27}H_{37}La$: C, 64.78; H, 7.47; La, 27.75. Found: C, 64.10; H, 7.62; La, 28.10. ^{1}H NMR (C_6D_{12}, 25 °C) δ 6.92 (t, 2H, *m*-CH$_2$C$_6$$H_5$), 6.55 (t, 1H, *p*-CH$_2C_6$$H_5$), 6.45 (d, 2H, *o*-CH$_2C_6$$H_5$), 2.22

(13) Evans, W. J.; Johnston, M. A.; Ziller, J. W. *Inorg. Chem.* **2000**, *39*, 3421.
(14) Evans, W. J.; Engerer, S. C.; Coleson, K. M. *J. Am. Chem. Soc.* **1981**, *103*, 6672.
(15) Evans, W. J.; Bloom, I.; Hunter, W. E.; Atwood, J. L. *J. Am. Chem. Soc.* **1983**, *105*, 1401.

Table 1. X-ray Data Collection Parameters for $[(C_5Me_5)_2Sm]_2[\mu\text{-}\eta^3\text{:}\eta^3\text{-}C(CH_2)_3]$, **1**, $[(C_5Me_5)_2La]_2[\mu\text{-}\eta^3\text{:}\eta^3\text{-}C(CH_2)_3]$, **2**, $[(C_5Me_5)_2Pr]_2[\mu\text{-}\eta^3\text{:}\eta^3\text{-}C(CH_2)_3]$, **3**, $[(C_5Me_5)_2Y]_2[\mu\text{-}\eta^3\text{:}\eta^3\text{-}C(CH_2)_3]$, **5**

empirical formula	$C_{44}H_{66}Sm_2$ **1**	$C_{44}H_{66}La_2\cdot C_7H_{14}$ **2**	$C_{44}H_{66}Pr_2\cdot C_7H_{14}$ **3**	$C_{44}H_{66}Y_2\cdot C_6H_{12}$ **5**
formula weight	895.67	970.97	974.97	856.94
temperature (K)	148(2)	163(2)	168(2)	163(2)
crystal system	monoclinic	triclinic	triclinic	triclinic
space group	$P2_1/c$	$P\bar{1}$	$P\bar{1}$	$P\bar{1}$
a (Å)	11.0444(12)	16.6276(13)	16.585(3)	10.9985(16)
b (Å)	21.716(2)	17.0288(14)	16.933(3)	14.343(2)
c (Å)	20.132(2)	17.8646(15)	17.790(3)	15.421(2)
α (deg)	90	100.2940(10)	100.103(3)	78.893(3)
β (deg)	101.143(2)	103.3710(10)	103.126(3)	74.856(3)
γ (deg)	90	92.617(2)	92.613(3)	76.397(2)
volume (Å^3)	4737.6(9)	4822.0(7)	4771.1(15)	2259.9(6)
Z	4	4	4	2
ρ_{calcd} (Mg/m^3)	1.256	1.337	1.357	1.259
μ (mm^{-1})	2.478	1.778	2.049	2.586
R1[a] ($I > 2.0\sigma(I)$)	0.0459	0.0402	0.0459	0.0512
wR2[b] (all data)	0.1508	0.1027	0.1114	0.1656

[a] $R1 = \Sigma||F_o| - |F_c||/\Sigma|F_o|$. [b] $wR2 = [\Sigma[w(F_o^2 - F_c^2)^2/\Sigma[w(F_o^2)^2]]^{1/2}$

(s, 2H, CH_2C$_6$H$_5$), 1.85 (s, 30H, C$_5$*Me*$_5$). ^{13}C NMR δ 11.24 (C$_5$*Me*$_5$), 32.50 (*C*H$_2$C$_6$H$_5$), 131.89, 128.98, 129.03 (CH$_2$*C*$_6$H$_5$), 127.94 (*C*$_5$Me$_5$). IR (thin film) 2961s, 2926s, 2876s, 1567w, 1459m, 1378m, 1343w, 1309w, 1262w, 1239w, 1069w, 1027w, 907w cm^{-1}.

X-ray Data Collection, Structure Solution, and Refinement. $[(C_5Me_5)_2Sm]_2[\mu\text{-}\eta^3\text{:}\eta^3\text{-}C(CH_2)_3]$, 1. An orange crystal of approximate dimensions 0.10 × 0.11 × 0.20 mm^3 was mounted on a glass fiber and transferred to a Bruker CCD platform diffractometer. The SMART[16] program package was used to determine the unit-cell parameters (Table 1) and for data collection (30 s/frame scan time for a sphere of diffraction data). The raw frame data were processed using SAINT[17] and SADABS[18] to yield the reflection data file. Subsequent calculations were carried out using the SHELXTL[19] program. The diffraction symmetry was 2/*m*, and the systematic absences were consistent with the centrosymmetric monoclinic space group $P2_1/c$ which was later determined to be correct.

The structure was solved by direct methods and refined on F^2 by full-matrix least-squares techniques. The analytical scattering factors[20] for neutral atoms were used throughout the analysis. Hydrogen atoms either were located from a difference Fourier map and refined (*x*,*y*,*z*, fixed U_{iso}) or were included using a riding model. The largest difference peaks are probably due to an unresolved methylcyclohexane solvent molecule. Least-squares analysis yielded wR2 = 0.1508 and GOF = 1.086 for 433 variables refined against 8968 data (0.82 Å). As a comparison for refinement on *F*, R1 = 0.0459 for those 6560 data with $I > 2.0\sigma(I)$.

$[(C_5Me_5)_2La]_2[\mu\text{-}\eta^3\text{:}\eta^3\text{-}C(CH_2)_3]$, 2. A yellow crystal of approximate dimensions 0.04 × 0.18 × 0.29 mm^3 was mounted on a glass fiber and handled as described for **1**. There were no systematic absences or any diffraction symmetry other than the Friedel condition. The centrosymmetric triclinic space group $P\bar{1}$ was assigned and later determined to be correct. There were two molecules of the formula unit present. There was also one molecule of methylcyclohexane solvent present per formula unit. At convergence, wR2 = 0.1027 and GOF = 1.033 were yielded for 921 variables refined against 19 440 data (0.80 Å). As a comparison for refinement on *F*, R1 = 0.0402 for those 13 605 data with $I > 2.0\sigma(I)$.

$[(C_5Me_5)_2Pr]_2[\mu\text{-}\eta^3\text{:}\eta^3\text{-}C(CH_2)_3]$, 3. A yellow crystal of approximate dimensions 0.05 × 0.17 × 0.32 mm^3 was mounted on a glass fiber and handled as described for **1**. There were no systematic absences nor any diffraction symmetry other than the Friedel condition. The centrosymmetric triclinic space group $P\bar{1}$ was assigned and later determined to be correct. The structure was solved using the coordinates of the lanthanum analogue, **2**, and refined on F^2 by full-matrix least-squares techniques. There were two independent molecules of the formula unit present ($Z = 4$) and one molecule of methylcyclohexane solvent per formula unit. At convergence, wR2 = 0.1114 and GOF = 1.035 were yielded for 921 variables refined against 16 241 data (0.80 Å). As a comparison for refinement on *F*, R1 = 0.0459 for those 10 364 data with $I > 2.0\sigma(I)$.

$[(C_5Me_5)_2Nd]_2[\mu\text{-}\eta^3\text{:}\eta^3\text{-}C(CH_2)_3]$, 4. A green crystal of approximate dimensions 0.05 × 0.12 × 0.27 mm^3 was mounted on a glass fiber and handled as described for **1**. The diffraction symmetry was 2/*m*, and the systematic absences were consistent with the centrosymmetric monoclinic space group $P2_1/c$ which was later determined to be correct.

The pentamethylcyclopentadienyl ligands were disordered and included using multiple components with partial site-occupancy factors. There was one molecule of methylcyclohexane solvent present. Least-squares analysis yielded wR2 = 0.1144 and GOF = 1.045 for 455 variables refined against 8172 data (0.85 Å). As a comparison for refinement on *F*, R1 = 0.0441 for those 5951 data with $I > 2.0\sigma(I)$.

$[(C_5Me_5)_2Y]_2[\mu\text{-}\eta^3\text{:}\eta^3\text{-}C(CH_2)_3]$, 5. A yellow crystal of approximate dimensions 0.10 × 0.21 × 0.30 mm^3 was mounted on a glass fiber and handled as described for **1**. There were neither systematic absences nor any diffraction symmetry other than the Friedel condition. The centrosymmetric triclinic space group $P\bar{1}$ was assigned and later determined to be correct. The structure was solved by direct methods and refined on F^2 by full-matrix least-squares techniques. There was one molecule of cyclohexane solvent present per formula unit. Least-squares analysis yielded wR2 = 0.1656 and GOF = 1.052 for 507 variables refined against 9203 data (0.80 Å). As a comparison for refinement on *F*, R1 = 0.0512 for those 7287 data with $I > 2.0\sigma(I)$.

$[(C_5Me_5)_2Sm]_2[\mu\text{-}(OCPh_2CH_2)_2C{=}CH_2)]$, 8. A yellow crystal of approximate dimensions 0.17 × 0.23 × 0.28 mm^3 was mounted on a glass fiber and handled as described for **1**. Details are in Table 2. The diffraction symmetry was 2/*m*, and the systematic absences were consistent with the centrosymmetric monoclinic space group $P2_1/c$ which was later determined to be correct. There were two molecules of the formula unit and two molecules of hexane solvent present. The distances within the hexane molecules were constrained during refinement. At convergence, wR2 = 0.1283 and GOF = 1.064 for 1447

(16) *SMART Software Users Guide*, version 5.1; Bruker Analytical X-Ray Systems, Inc.: Madison, WI, 1999.
(17) *SAINT Software Users Guide*, version 6.0; Bruker Analytical X-Ray Systems, Inc.: Madison, WI, 1999.
(18) Sheldrick, G. M. *SADABS*, version 2.10; Bruker Analytical X-Ray Systems, Inc.: Madison, WI, 2002.
(19) Sheldrick, G. M. *SHELXTL*, version 6.12; Bruker Analytical X-Ray Systems, Inc.: Madison, WI, 2001.
(20) *International Tables for X-Ray Crystallography*; Kluwer Academic Publishers: Dordrecht, 1992; Vol. C.

Table 2. X-ray Data Collection Parameters for $[(C_5Me_5)_2Sm]_2[\mu\text{-}(OCPh_2CH_2)_2C{=}CH_2)]$, **8**

empirical formula	$C_{70}H_{86}O_2Sm_2{\cdot}C_6H_{14}$ **$8{\cdot}C_6H_{14}$**
formula weight	1346.26
temperature (K)	158(2)
crystal system	monoclinic
space group	$P2_1/c$
a (Å)	18.417(2)
b (Å)	21.606(2)
c (Å)	35.253(3)
α (deg)	90
β (deg)	105.023(2)
γ (deg)	90
volume (Å^3)	13548(2)
Z	8
ρ_{calcd} (Mg/m^3)	1.320
μ (mm^{-1})	1.760
R1[a] ($I > 2.0\sigma(I)$)	0.0434
wR2[b] (all data)	0.1283

[a] $R1 = \Sigma||F_o| - |F_c||/\Sigma|F_o|$. [b] $wR2 = [\Sigma[w(F_0^2 - F_c^2)^2/\Sigma[w(F_o^2)^2]]^{1/2}$.

variables refined against 27 683 data (0.80 Å). As a comparison for refinement on F, R1 = 0.0434 for those 20 440 data with $I > 2.0\sigma(I)$.

Computational Details. All calculations were performed with the Gaussian 03 code.[21] For the carbon atoms of the TMM unit and all the hydrogen atoms, the 6-31G** basis set was employed. For the ring C atoms, the "SDDALL" pseudopotential and basis set of the Stuttgart−Bonn variety was employed, supplemented with a d polarization function with the exponent = 0.8. For the La and Lu atoms the small-core Stuttgart−Bonn pseudopotential was employed, together with the (14s13p10d8f)/[10s8p5d4f] segmented valence basis set of Cao and Dolg[22] (note that the g functions were deleted from the original basis set). The PBE gradient corrected functional was employed. Natural charges and populations were obtained with NBO version 3.1.[23] The structural and orbital pictures were generated using the GaussView code.

Results

Synthesis. $[(C_5Me_5)_2Ln]_2[\mu\text{-}\eta^3{:}\eta^2\text{-}C(CH_2)_3]$ complexes of La, **2**, Pr, **3**, and Nd, **4**, analogous to the Sm complex, **1**, reported earlier[2] can be made from the corresponding tetraphenylborate salts, $[(C_5Me_5)_2Ln][(\mu\text{-}Ph_2)BPh_2]$[8] and neopentyl lithium according to eq 2. The reaction sequence is presumably the same as that demonstrated for samarium in Scheme 1. The isolation of the lanthanum complex, **2**, allowed structural data to be obtained on a closed shell complex, thereby allowing direct comparison with density functional theory calculations.

A second route to the four-carbon ligands in the TMM complexes was examined using a more "atom efficient" route involving the four-carbon precursor, isobutyl lithium, as outlined in Scheme 2. In this case, β-hydride rather than β-alkyl elimination would provide the necessary isobutene for subsequent metalation. The metalation could occur via the metallocene hydride formed in the β-hydride elimination,[24] but the $(C_5Me_5)_2Ln(CH_2CHMe_2)$ intermediate would be expected to be the more powerful metalation reagent.[1,25−27] When this route was tried with lanthanum and samarium, the TMM complexes **1** and **2** were in fact isolated. However, in no case did this isobutyl route give high yields of the TMM products. Hence, this did not prove to be a better route to these compounds with these metals.

The isolation of TMM complexes from $[(C_5Me_5)_2Ln][(\mu\text{-}Ph_2)BPh_2]$ and isobutyl lithium does provide evidence for the existence of the isobutyl lanthanide metallocenes, "$[(C_5Me_5)_2Ln(CH_2CHMe_2)]_x$". These complexes would be expected to be exceptionally reactive via β-H elimination to form the isobutene necessary for subsequent metalation to the $[C(CH_2)_3]^{2-}$ ligand as shown in the first reaction in Scheme 2. If the $[(C_5Me_5)_2LnH]_x$ product of that reaction did a subsequent metalation as shown in eq 3, the formation of hydrogen in the system would be expected. This was not observed, but instead isobutane was

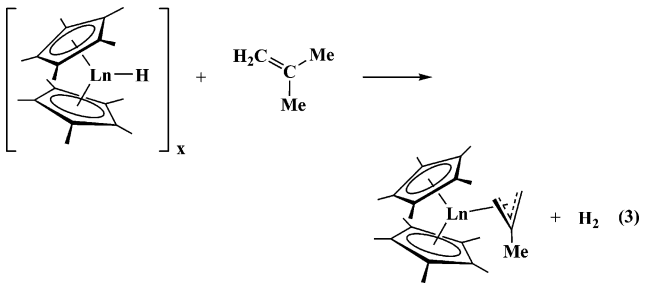

(3)

found. This is consistent with the metalation of isobutene by "$[(C_5Me_5)_2Ln(CH_2CHMe_2)]_x$" as shown in the third reaction in Scheme 2. Likewise the absence of hydrogen suggests that the metalation of the methyl-allyl complex to form the TMM complex, the last reaction in Scheme 2, was also done with "$[(C_5Me_5)_2Ln(CH_2CHMe_2)]_x$" and not $[(C_5Me_5)_2LnH]_x$. The overall reaction for the formation of the TMM complexes by this isobutyl route is shown in eq 4.

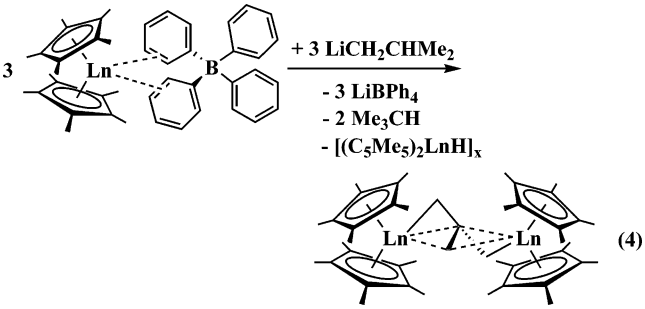

(4)

Attempts to make the Y and Lu analogues of **1**−**4** from $LiCH_2CMe_3$ and $LiCH_2CHMe_2$ under identical reaction conditions were unsuccessful. In the lutetium case, evidence for a stable neopentyl complex, "$[(C_5Me_5)_2Lu(CH_2CMe_3)]_x$", **7**, was found. Specifically, yellow crystalline material was isolated from the reaction of $[(C_5Me_5)_2Lu][(\mu\text{-}Ph_2)BPh_2]$ and neopentyl lithium as shown in eq 5 that matched the composition "$[(C_5Me_5)_2Lu(CH_2CMe_3)]_x$" by complete elemental analysis and by NMR spectroscopy. The ^{1}H NMR spectrum contained only a reso-

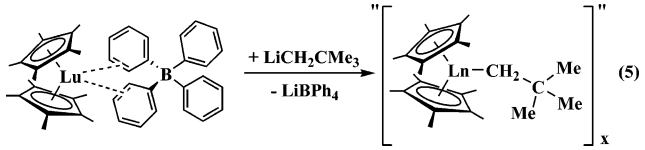

(5)

nance of 30 at 1.96 ppm attributed to $(C_5Me_5)^{1-}$ and resonances of 9 and 2 at 0.99 and 0.22 ppm, respectively, consistent with a neopentyl group. The ^{13}C NMR spectrum contained resonances

(21) Frisch, M. J., et al. *Gaussian 03*, revision C.2; Gaussian Inc.: Wallingford, CT, 2004
(22) Cao, X. Y.; Dolg, M. *J. Mol. Struct.* **2002**, *581*, 139.
(23) Glendening, E. D.; Reed, A. E.; Carpenter, J. E.; Weinhold, F. *NBO*, version 3.1.
(24) Evans, W. J.; Ulibarri, T. A.; Ziller, J. W. *Organometallics* **1991**, *10*, 134.
(25) Watson, P. L.; Parshall, G. W. *Acc. Chem. Res.* **1985**, *18*, 51.
(26) Sadow, A. D.; Tilley, T. D. *J. Am. Chem. Soc.* **2003**, *125*, 7971.
(27) Thompson, M. E.; Bercaw, J. E. *Pure Appl. Chem.* **1984**, *56*, 1.

Scheme 2

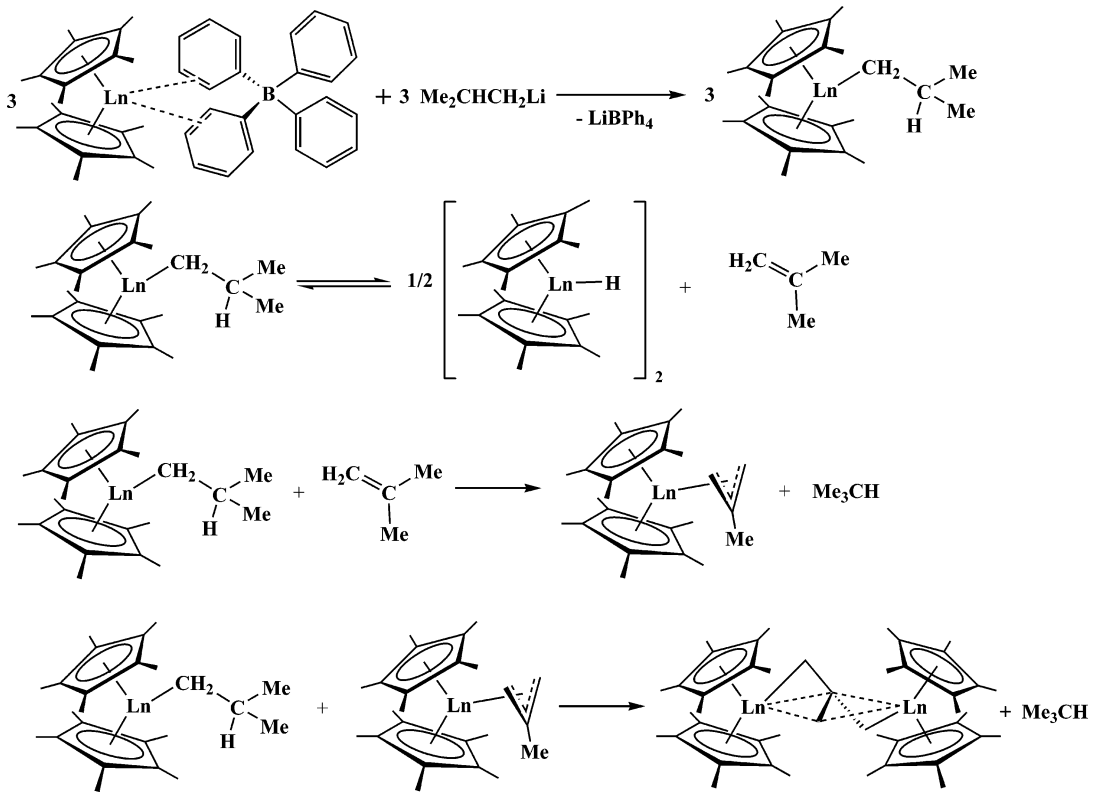

at 10.9 and 118.4 ppm for the $(C_5Me_5)^{1-}$ carbons. The methylene and methyl carbon resonances of the neopentyl ligand were located at 49.1 and 29.4 ppm, but the quaternary carbon was not located. Evidence for the existence of $[(C_5Me_5)_2Y(CH_2CHMe_2)]_x$ at low temperature and $[(C_5Me_5)_2Lu(CH_2CHMe_2)]_x$ has been previously reported.[28,29]

Heating a sample of **7** did not lead to a TMM analogue of **1**−**5** but rather formed only the β-Me elimination product, $[(C_5Me_5)_2LuMe]_x$, eq 6.[1,29−31] This complex was identified by ^{1}H

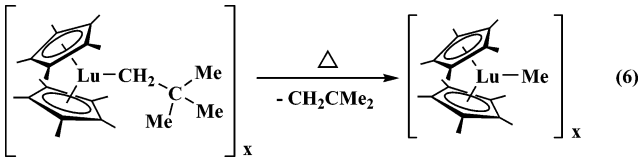

(6)

NMR spectroscopy and X-ray crystallography. Attempts to isolate an yttrium neopentyl complex, $[(C_5Me_5)_2Y(CH_2CMe_3)]_x$, analogous to the lutetium complex resulted only in the formation of the known $[(C_5Me_5)_2YMe]_x$.[25]

Since neither eq 2 nor eq 4 led to TMM complexes of Y and Lu, an alternative route was examined starting with the methylallyl intermediates in Schemes 1 and 2. The required yttrium methylallyl complex, $(C_5Me_5)_2Y[CH_2C(Me)CH_2]$, **6**, could be obtained in good yield from the reaction of $(C_5Me_5)_2Y(\mu\text{-}Cl)_2K(THF)_2$ with $[CH_2C(Me)CH_2]MgCl$, eq 7. Metalation of **6** with $[(C_5Me_5)_2YH]_x$ provided a fully characterizable yttrium TMM complex, $[(C_5Me_5)_2Y]_2[\mu\text{-}\eta^3\text{:}\eta^3\text{-}C(CH_2)_3]$, **5**, eq 8.

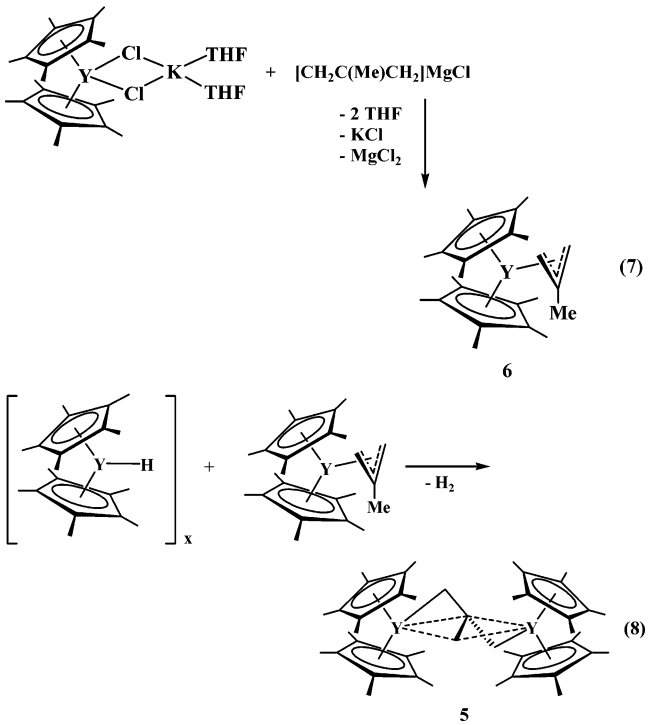

(7)

(8)

Structural Analysis. The X-ray crystal structures of **2**−**5** were obtained for comparison with the structure of **1**, Figure 2. The five complexes **1**−**5** are isomorphous and have similar metrical parameters as shown in Table 3. Both the lanthanum and samarium complexes have disorder in one $(C_5Me_5)^{1-}$ ligand,

(28) Casey, C. P.; Tunge, J. A.; Lee, T.-Y.; Carpenetti, D. W., III. *Organometallics* **2002**, *21*, 389.
(29) Watson, P. L.; Roe, C. D. *J. Am. Chem. Soc.* **1982**, 6471.
(30) Watson, P. L. *J. Am. Chem. Soc.* **1982**, 337.
(31) Watson, P. L. *J. Am. Chem. Soc.* **1983**, 6491.

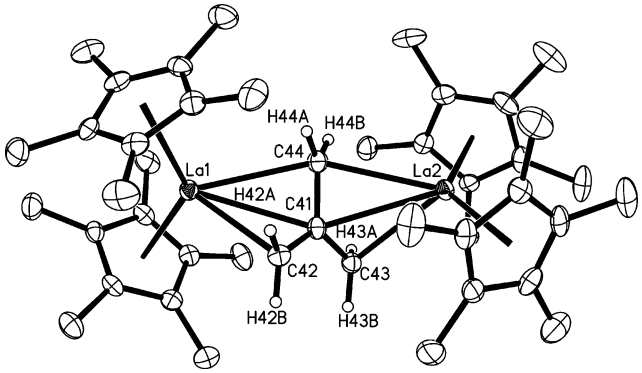

Figure 2. Thermal ellipsoid plot of $[(C_5Me_5)_2La]_2[\mu\text{-}\eta^3\text{:}\eta^3\text{-}C(CH_2)_3]$, **2**, with the probability ellipsoids drawn at the 50% level. Methyl hydrogen atoms have been excluded for clarity.

and the neodymium complex did not provide high quality data. These problems were not found in the praseodymium complex. The fact that the best crystallographic data without disorder could be obtained with Pr but not with the analogues slightly larger or smaller emphasizes the subtleties of varying the size of the lanthanide metal within a given ligand set.

The $[C(CH_2)_3]^{2-}$ dianions in **2**−**5** adopt a planar bridging coordination mode like that of **1**, A in Scheme 3. This differs from those previously observed for TMM metal complexes, B−D,[32−35] Scheme 3. The TMM ligands are planar to within 0.003 Å in the crystallographically well resolved complexes **1**−**3** and **5**. A $\mu\text{-}\eta^3\text{:}\eta^3$ mode of attachment to the metals is found in each case.

The data in Table 3 allow a detailed comparison of the TMM bonding in lanthanide complexes with three different $4f^n$ electron configurations. Examination of the Ln−C(C_5Me_5) average bond distances for $4f^5$ Sm^{3+}, $4f^3$ Pr^{3+}, and $4f^0$ La^{3+}, 2.733(5), 2.771(7), and 2.818(7) Å, shows that these change as expected based on the differences in ionic radii of these metals: the Shannon radius for Pr^{3+} is 0.047 Å larger than that for Sm^{3+}, and the Shannon radius for La^{3+} is 0.037 Å larger than that for Pr^{3+}. All of the Ln−C(TMM) distances also vary in this order, La^{3+} > Pr^{3+} > Sm^{3+}. In most cases, the differences in these Ln−C(TMM) lengths match the differences in the ionic radii; i.e., for each analogous measurement they differ by 0.04−0.05 Å. The only exceptions are the La(1)−C(41) and La(1)−C(44) distances, which are only 0.02 Å larger than their Pr analogues, and Sm(2)−C(44), which is only 0.02 Å shorter than the Pr analogue. These variations are probably within the error limits of the measurements.

Scheme 3

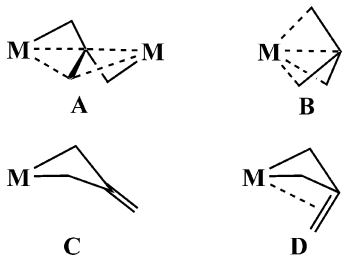

The structure of the yttrium analogue, **5**, provides another basis of comparison, in this case with a $4d^0$ system. As shown in Table 3, the metrical data on the yttrium system also coincide with those of **1**−**3** when the differences in ionic radii are considered, i.e., the yttrium distances are typically 0.14 Å shorter than those for lanthanum. This is typical of Y^{3+} complexes since this ion is similar in size to the late lanthanides, Ho^{3+} and Er^{3+}, and its complexes resemble late lanthanide analogues in both reactivity and structure.

Table 3. Bond Distances (Å) and Angles (deg) in $[(C_5Me_5)_2Sm]_2[\mu\text{-}\eta^3\text{:}\eta^3\text{-}C(CH_2)_3]$, **1**, $[(C_5Me_5)_2La]_2[\mu\text{-}\eta^3\text{:}\eta^3\text{-}C(CH_2)_3]$, **2**, $[(C_5Me_5)_2Pr]_2[\mu\text{-}\eta^3\text{:}\eta^3\text{-}C(CH_2)_3]$, **3**, and $[(C_5Me_5)_2Y]_2[\mu\text{-}\eta^3\text{:}\eta^3\text{-}C(CH_2)_3]$, **5**

bond distances/angles	Sm, **1**	Pr, **3**	La, **2**	La calcd	Y, **5**	Lu calcd
Ln(1)−Cnt	2.454/2.454	2.487/2.512	2.538/2.559	2.591	2.392	2.370
Ln(2)−Cnt	2.439/2.467	2.484/2.508	2.537/2.562	2.572	2.366	2.330
Ln(1)−C(C_5Me_5) avg	2.733(5)	2.771(7)	2.818(7)	2.854	2.666(7)	2.628
Ln(1)−C(41)	2.799(4)	2.841(7)	2.858(5)	2.887	2.719(5)	2.732
Ln(1)−C(44)	2.745(4)	2.800(8)	2.824(5)	2.836	2.641(6)	2.690
Ln(1)−C(42)	2.546(4)	2.618(8)	2.648(5)	2.664	2.472(6)	2.462
Ln(2)−C(41)	2.793(4)	2.830(7)	2.870(5)	2.887	2.698(5)	2.732
Ln(2)−C(44)	2.734(4)	2.752(8)	2.795(5)	2.836	2.672(6)	2.690
Ln(2)−C(43)	2.567(4)	2.617(8)	2.659(5)	2.664	2.500(6)	2.461
C(41)−C(42)	1.432(6)	1.418(10)	1.415(7)	1.437	1.427(8)	1.442
C(41)−C(43)	1.426(6)	1.414(10)	1.412(6)	1.437	1.452(8)	1.442
C(41)−C(44)	1.424(6)	1.422(10)	1.430(7)	1.447	1.406(9)	1.449
Cnt1−Ln(1)−Cnt2	133.6	134.0	134.1		134.3	
Cnt3−Ln(2)−Cnt4	134.1	134.6	134.8		133.5	
Cnt1−Ln(1)−C(42)	107.9	108.9	109.2		110.9	
Cnt1−Ln(1)−C(41)	105.4	106.9	107.4		102.8	
Cnt1−Ln(1)−C(44)	121.7	123.3	124.4		121.7	
Cnt2−Ln(1)−C(42)	109.2	107.8	106.8		107.4	
Cnt2−Ln(1)−C(41)	120.7	118.7	117.9		118.7	
Cnt2−Ln(1)−C(44)	102.3	100.7	99.9		104.0	
Cnt3−Ln(2)−C(43)	108.1	107.4	106.4		109.8	
Cnt3−Ln(2)−C(41)	120.1	118.9	118.3		121.2	
Cnt3−Ln(2)−C(44)	102.4	101.3	101.4		101.1	
Cnt4−Ln(2)−C(43)	108.3	107.5	107.6		108.6	
Cnt4−Ln(2)−C(41)	105.4	105.7	105.8		105.3	
Cnt4−Ln(2)−C(44)	121.3	122.7	122.7		121.8	
C(42)−C(41)−C(43)	124.2(4)	123.4(7)	123.8(5)	123.9	123.4(5)	
C(42)−C(41)−C(44)	117.5(4)	118.6(7)	118.2(4)	118.0	118.7	
C(43)−C(41)−C(44)	118.3(4)	118.0(7)	118.0(4)	118.0	117.9	

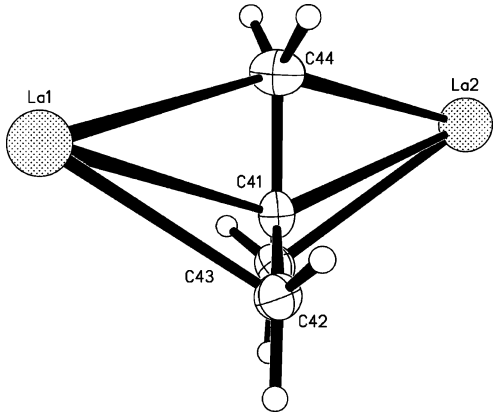

Figure 3. $Ln_2[\mu\text{-}\eta^3\text{:}\eta^2\text{-}C(CH_2)_3]$ core structure in **2**.

In contrast to these metal radius based variations in Ln−C bonds, the C−C bonds of the TMM ligands in **1**−**3** are identical within experimental error. All of the C−C bonds are in the narrow range 1.412(6)−1.432(6) Å. The C−C−C angles in the TMM ligands are also equivalent within experimental error. The C−C distances in yttrium analogue **5** span a wider range, 1.406(9)−1.452(8) Å, but are still equivalent within experimental error.

In the case of **2** and **3**, hydrogen positions were located in the X-ray data although the C−H distances and thermal parameters were fixed during refinement. Figure 3 shows the positions of the hydrogen atoms of the TMM ligand in **2** according to this model. As shown, only two of the six hydrogens lie directly in the C4 plane in this refinement model. Interestingly, the DFT calculations (see below) on the La complex **2** also suggest that two of the six hydrogen atoms lie in the C4 plane. Of the remainder, two hydrogens are 20° out of the plane, while the final two are 33° out.

Density Functional Theory Analysis. The initial X-ray crystallographic data on **1** were obtained on a crystal that contained methylcyclohexane solvent. The TMM ligand had one C(central)−C(methylene) distance shorter than the others: 1.351(16) Å C(41)−C(44) vs 1.464(16) Å C(41)−C(42) and 1.474(16) Å C(41)−C(43). These bond distances are similar to those in $(C_5Me_5)_2Zr[\eta^2\text{-}C(CH_2)_3]$ (137.6(9), 1.49(1), and 1.51(1) Å), which has structure C, Scheme 3.[4] Hence, the TMM ligand in **1** appeared to have a localized structure in which C(41)−C(44) was a double bond and C(42) and C(43) were two $(CH_2)^{1-}$ substituents.

DFT calculations on **1** were attempted with the aim of rationalizing the apparently localized bonding within the TMM ligand. The starting geometry was taken from the crystallographic data, ensuring that the orientation of the TMM unit was comparable with that determined experimentally. This orientation was also adopted for subsequent calculations on the La and Lu systems. However, the presence of two open $4f^5$ configurations precluded satisfactory SCF and geometry convergence. To avoid the open shell problem, calculations on the analogous closed shell complex $[(C_5Me_5)_2La]_2[\mu\text{-}\eta^3\text{:}\eta^3\text{-}C(CH_2)_3]$,

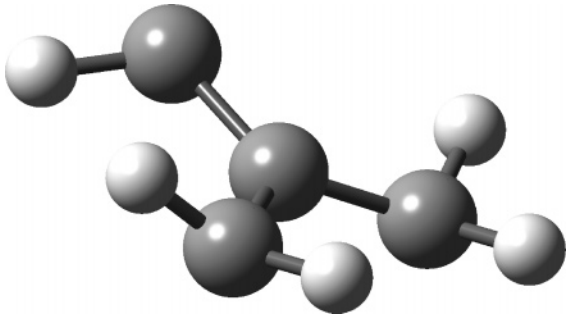

Figure 4. Ball−stick representation of the optimized geometry of $[C(CH_2)_3]^{2-}$.

2, were performed. As expected, calculations on **2** proceeded more smoothly than those on **1** but produced a geometry significantly different from that obtained from the crystal of **1** with methylcyclohexane solvent. As shown in Table 3, the DFT calculation predicted a delocalized structure for the TMM unit.

Since the X-ray data on the crystal of **1** containing methylcyclohexane had a rather high wR2 value of 0.1396 and had all carbon atoms disordered except the C(41)−C(44) carbons of the TMM ligand, a second crystal of **1** was examined. In this case, a crystal containing cyclohexane solvent was isolated. This crystal gave data with wR2 = 0.0602 and showed that the TMM ligand indeed did have a delocalized structure with 1.424(6) Å C(41)−C(44), 1.432(6) Å C(41)−C(42), and 1.426(6) Å C(41)−C(43), distances that are indistinguishable. This sequence of events is an excellent illustration of the role that theory can play in guiding experiment to a more reliable result.

Following the two data collections on **1**, a third data set was collected as part of this study and is consistent with the second data set; i.e., a delocalized TMM structure was found. The X-ray crystal structures of analogues with other metals, **2**−**5**, are similar.

With the X-ray data on **2** available, a direct comparison of theory and experiment can be made with the same metal. The results are shown in Table 3 and reveal that the calculation generally matches the structure but overestimates slightly the La−C(TMM) distances, as well as those between the metal and the C_5Me_5 rings.[36] The experimental patterns of (a) La(1)−C(41) > La(1)−C(44) ≫ La(1)−C(42) and (b) La(2)−C(41) > La(2)−C(44) ≫ La(2)−C(43) are also found computationally. Within the TMM unit, the experimental pattern of C(41)−C(42) ≈ C(41)−C(43) < C(41)−C(44) is well reproduced by the calculation, although computation overestimates the C−C bond lengths by about 0.02 Å. Clearly, the experimental and theoretical structural evidence strongly point to a delocalized bonding mode within the TMM ligand.

The TMM unit carries a formal 2-charge in **1**−**5**. Geometry optimization of singlet $[C(CH_2)_3]^{2-}$ proceeded smoothly to a structure very similar to that first noted as the most stable form by Frenking et al.[7] The structure is shown in Figure 4 and

(32) Jones, M. D.; Kemmitt, R. D. W. *Adv. Organomet. Chem.* **1987**, *27*, 279.
(33) Albright, T. A.; Hofmann, P.; Hoffmann, R. *J. Am. Chem. Soc.* **1977**, *99*, 7546.
(34) Bazan, G. C.; Rodriguez, G.; Cleary, B. P. *J. Am. Chem. Soc.* **1994**, *116*, 2177.
(35) Keaton, R. J.; Koterwas, L. A.; Fettinger, J. C.; Sita, L. R. *J. Am. Chem. Soc.* **2002**, *124*, 5932.

(36) To probe the effect of basis set, the optimizations of **2** and the Lu analogue were repeated using the all-electron 6-31G** basis for the C and H atoms, together with the large core metal ECPs and associated basis sets (in which the 4f orbitals are treated as part of the core). While the distances within the TMM unit were largely unaffected (the largest difference being a 0.004 Å increase in C(41)−C(44) in **2**), those between the metal and the TMM carbon atoms were 0.03−0.04 Å longer with the new basis set in both molecules. Furthermore, the average La−C(C_5Me_5) distance increased by 0.03 Å, and that for Lu−C(C_5Me_5), by 0.07 Å. The new basis set combination clearly does a poorer job of reproducing all of the La−C distances in **2** than does our original choice.

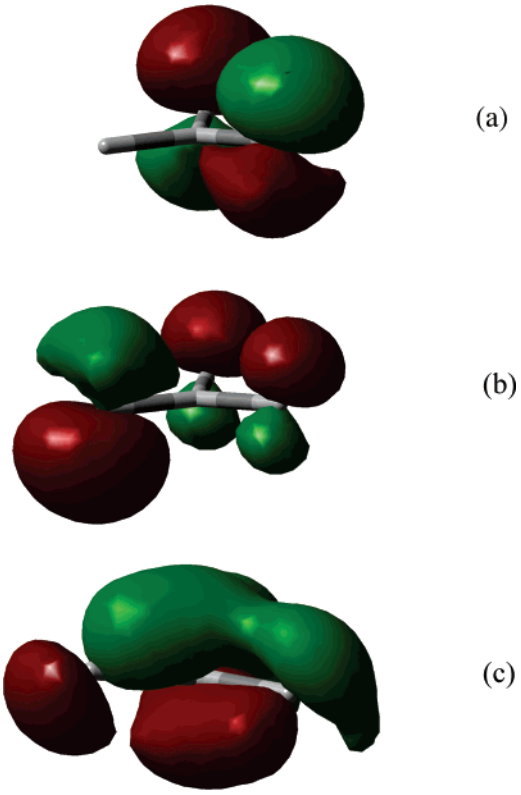

Figure 5. Three-dimensional isosurface representations (isoval = 0.05) of the (a) HOMO, (b) HOMO-1, and (c) HOMO-2 of $C(CH_2)_3^{2-}$. Hydrogen atoms have been excluded for clarity.

Table 4. Natural Atomic Charges and Electron Populations for the La, Lu, and TMM C Atoms in $[(C_5Me_5)_2La]_2[\mu\text{-}\eta^3\text{:}\eta^3\text{-}C(CH_2)_3]$, **2**, and $[(C_5Me_5)_2Lu]_2[\mu\text{-}\eta^3\text{:}\eta^3\text{-}C(CH_2)_3]$

		natural electron population					
atom	charge	4f	5d	5f	6s	6p	6d
La (1 and 2)	+2.421	0.15	0.33	0.02	0.07	0.01	0.01
Lu (1 and 2)	+1.836	13.99	0.94	0.00	0.12	0.01	0.11
C41 (La)	−0.158						
C41 (Lu)	−0.072						
C42 (La)	−0.919						
C42 (Lu)	−0.859						
C43 (La)	−0.919						
C43 (Lu)	−0.859						
C44 (La)	−1.015						
C44 (Lu)	−0.884						

features significant pyramidalization at the terminal carbon atoms. This structure is 9.5 kcal mol^{-1} more stable than that of $[C(CH_2)_3]^{2-}$ at its geometry in the optimized structure of **2**. The highest three occupied molecular orbitals of ground state $[C(CH_2)_3]^{2-}$ are shown in Figure 5. They contain significant π character, with the σ orbitals (not shown) lying below them energetically.

Analysis of the electronic structure of **2** at its optimized geometry reveals that the bonding between the metal atoms and the TMM unit is very ionic. The natural charges on the La atoms and the C atoms of the TMM ligand are given in Table 4, together with the natural electron configurations of the La. Given that calculated charges are rarely, if ever, as high as formal ones, the computed +2.421 for the La and −1.573 for the TMM unit provide good evidence for a largely ionic metal−ligand interaction.

This is reinforced upon examination of the MOs of **2**. The HOMO (MO 154, at −4.03 eV) and HOMO−1 (MO 153, at −4.19 eV) are shown in Figure 6a and 6b and feature major contributions from, respectively, the HOMO and HOMO−1 of optimized $[C(CH_2)_3]^{2-}$. Below these two orbitals comes a group of eight MOs, spanning a small energy range from −4.45 eV to −4.80 eV, which are primarily C_5Me_5 π_1 in character (i.e., they consist of combinations of the ring pπ orbitals with one vertical node). The exception is MO 147, at −4.71 eV, shown in Figure 6c, which is the only MO to demonstrate significant La−TMM covalency. This orbital features $[C(CH_2)_3]^{2-}$ HOMO−1 character, together with some La 5d content. Below these eight orbitals is a 2.21 eV gap to the next level, MO 144, which is reminiscent of the $[C(CH_2)_3]^{2-}$ HOMO−2 (Figure 6d).

Thus the picture that emerges from the analysis of the La−TMM bonding in **2** is consistent with the standard view of lanthanum chemistry. Each La atom gives up an electron to each of its C_5Me_5 ligands, and a third, to the TMM unit. The bonding is largely ionic, with only small indications of covalency.

A geometry optimization was also performed on $[(C_5Me_5)_2Lu]_2[\mu\text{-}\eta^3\text{:}\eta^3\text{-}C(CH_2)_3]$, using the structure of **2** as an initial guess. The geometry converged slowly but smoothly to a structure very similar to that of the La compound. The principal bond lengths of the optimized Lu structure are collected in Table 3. All of the Lu−C distances are shorter than the analogous La values, by around 8% for the average Lu−C(C_5Me_5), Lu(1)−C(42), and Lu(2)−C(43) and by around 5% for the rest, a clear example of the lanthanide contraction. Within the TMM unit, the distances are very similar to those in the La system, although the small difference between C(41)−C(42)/C(41)−C(43) and C(41)−C(44) is even less in the Lu compound. Thus the calculated structural data strongly suggest that the bonding within the TMM unit in $[(C_5Me_5)_2Lu]_2[\mu\text{-}\eta^3\text{:}\eta^3\text{-}C(CH_2)_3]$ is, as in **2**, delocalized.

Examination of the valence MOs of $[(C_5Me_5)_2Lu]_2[\mu\text{-}\eta^3\text{:}\eta^3\text{-}C(CH_2)_3]$ shows them to be very similar to those of **2**. As with **2** there are two closely spaced levels (the analogues of MO 154 and 153 in **2**) which form the HOMO and HOMO−1, which look very similar to Figure 6a and 6b, although in $[(C_5Me_5)_2Lu]_2[\mu\text{-}\eta^3\text{:}\eta^3\text{-}C(CH_2)_3]$ the ordering of these two orbitals is reversed. Once again there is then a group of eight closely spaced orbitals of predominant C_5Me_5 π_1 character, before a >2 eV gap to the next level, the analogue of MO 144 in **2** (Figure 6d). Within the group of eight C_5Me_5 π_1-based orbitals comes MO 163, the equivalent of MO 147 in **2**, and the isosurfaces of these orbitals are virtually superimposable.

Thus the picture of the metal−ligand bonding in $[(C_5Me_5)_2Ln]_2[\mu\text{-}\eta^3\text{:}\eta^3\text{-}C(CH_2)_3]$ that emerges from examination of the MO structure of the La and Lu systems is that it is very similar at the two ends of the 4f block. However, the natural charge and population analyses reveal some differences between the La and Lu compounds, as can be seen in Table 4. It is noticeable that the small 4f population seen in **2** has disappeared in $[(C_5Me_5)_2Lu]_2[\mu\text{-}\eta^3\text{:}\eta^3\text{-}C(CH_2)_3]$, presumably because the 4f orbitals are so contracted by the end of the lanthanide series as to be entirely corelike. By contrast, there is a significantly larger 5d population in the Lu system than in the La, and this is reflected in the charge on the Lu atoms, which is 0.585 less than that on the La. Indeed, the natural charges suggest that the metal−TMM

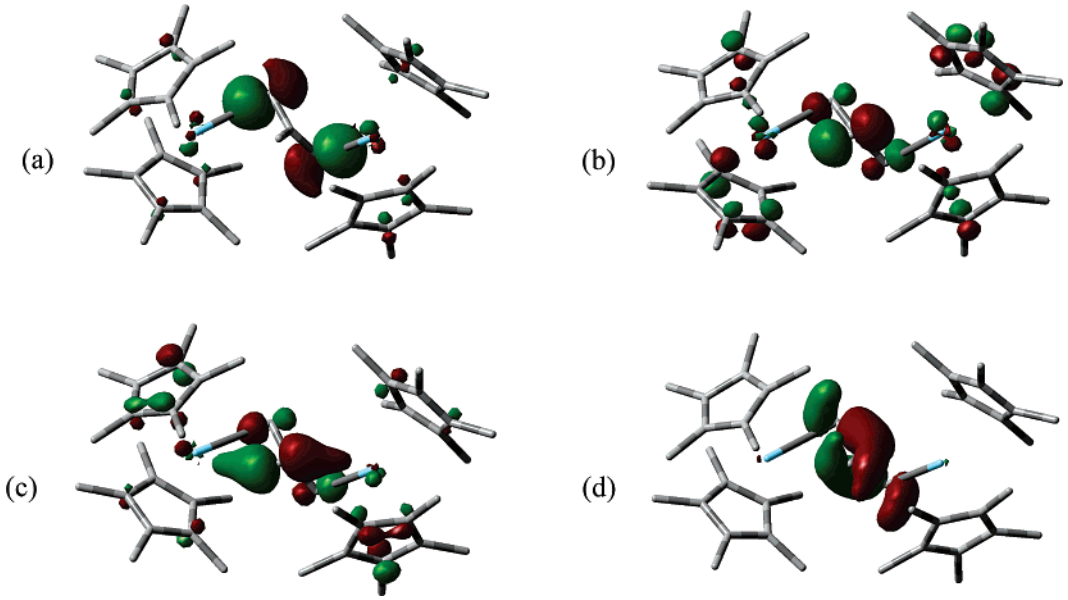

Figure 6. Three-dimensional isosurface representations (isoval = 0.05) of (a) the HOMO (MO 154), (b) the HOMO-1 (MO 153), (c) MO 147, and (d) MO 144 of $[(C_5Me_5)_2La]_2[\mu\text{-}\eta^3\text{:}\eta^3\text{-}C(CH_2)_3]$, **2**. Hydrogen atoms have been excluded for clarity.

bonding in the Lu compound is less polar than that in **2**, although given that the charge difference between the Lu atoms and the TMM unit is around 3, the bonding must still be regarded as very ionic. That the metal−ligand bonding in both **2** and the Lu system is predominantly ionic is consistent with the well-established view of Ln(III) chemistry.[37−40] These differences between La and Lu are consistent with the fact that La is the lanthanide closest to Ba and Lu is the lanthanide closest to Hf. Hence, it is reasonable that La is more like the ionic alkali metals and alkaline earths and Lu displays more d character like its nearby transition metal neighbors.

Reactivity. The reactivity of the bimetallic lanthanide metallocene TMM complexes with benzophenone was examined to make a comparison with the insertion reaction observed with the mixed ligand zirconium complex, $(C_5Me_5)[^iPrNC(Me)N^i\text{-}Pr]Zr[C(CH_2)_3]$, eq 9.[3] In that case, benzophenone inserted

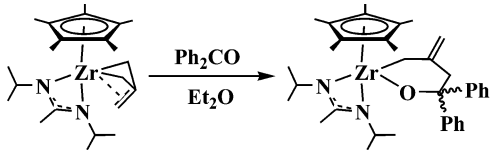

(9)

to make a bidentate alkyl alkoxide ligand, $[OCPh_2CH_2C(=CH_2)CH_2]^{2-}$. Complex **1** reacts similarly with benzophenone, but since **1** is bimetallic, two benzophenone molecules insert in this case to form $[(C_5Me_5)_2Sm]_2[\mu\text{-}(OCPh_2CH_2)_2C{=}CH_2]$, **8**, eq 10, Figure 7. Attempts to isolate a product from a single insertion of Ph_2CO were unsuccessful and only gave a lower yield of **8**.

Complex **8** contains one formally seven-coordinate metal center [Sm(2)] and one with higher coordination due to a 3.012(6) Å long distance interaction between the vinyl carbon, C(42),

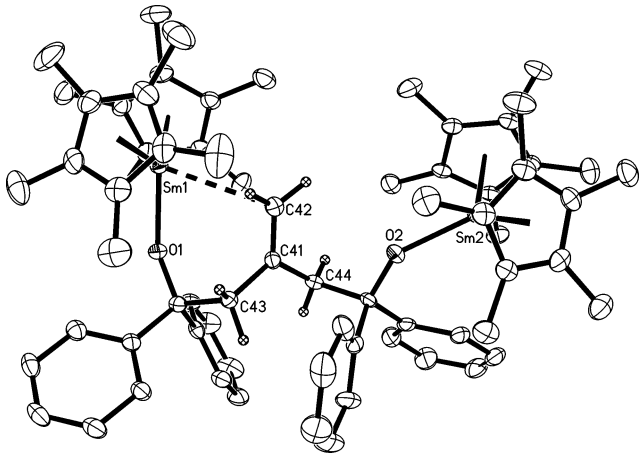

Figure 7. Thermal ellipsoid plot of $[(C_5Me_5)_2Sm]_2[\mu\text{-}(OCPh_2)_2C(CH_2)_3]$, **8**, with the probability ellipsoids drawn at the 50% level. Methyl and phenyl hydrogen atoms have been excluded for clarity.

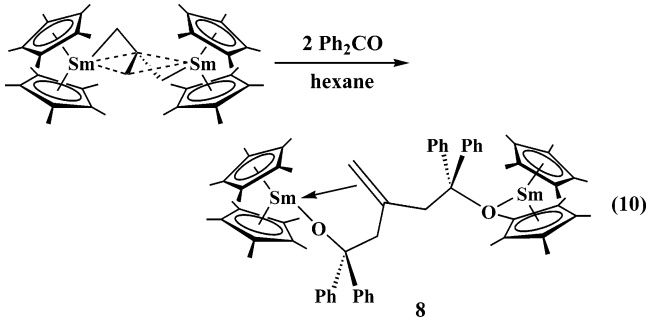

(10)

and Sm(1). The distance between these two atoms is long compared to the Sm−C(C_5Me_5) lengths (Table 5) that range from 2.686(5) to 2.808(6) Å for Sm(1) and 2.701(5) to 2.786(5) Å for Sm(2). As shown by these ranges and the (C_5Me_5 ring centroid)−Sm lengths for Sm(1), 2.479 and 2.474 Å, and Sm(2), 2.444 and 2.467 Å, the effect of the long distance Sm(1)−C(42) interaction on the metallocene moieties is minimal. Similarly, the 2.136(4) Å Sm(1)−O(1) and 2.145(4) Å Sm(2)−O(2) lengths are within experimental error.

(37) Mehdoui, T.; Berthet, J.-C.; Thuéry, P.; Ephritikhine, M. *Dalton Tran.* **2005**, *7*, 1263.
(38) Karmazin, L.; Mazzanti, M.; Bezombes, J.-P.; Gateau, C.; Pécaut, J. *Inorg. Chem.* **2004**, *43*, 5147.
(39) Gaunt, A. J.; Scott, B. L.; Neu, M. P. *Angew. Chem., Int. Ed.* **2006**, *45*, 1638.
(40) Perrin, L.; Maron, L.; Eisenstein, O. *Faraday Discuss.* **2003**, *124*, 25.

Table 5. Bond Distances (Å) and Angles (deg) in $[(C_5Me_5)_2Sm]_2[\mu\text{-}(OCPh_2CH_2)_2C{=}CH_2)]$, **8**

bond distances/angles	8
Ln(1)−Cnt	2.479/2.474
Ln(2)−Cnt	2.444/2.467
Ln(1)−C(C_5Me_5) avg	2.754(4)
Ln(2)−C(C_5Me_5) avg	2.735(3)
Ln(1)−O(1)	2.136(4)
Ln(2)−O(2)	2.145(4)
C(41)−C(42)	1.339(8)
C(41)−C(43)	1.510(7)
C(41)−C(44)	1.511(7)
Ln(1)−C(42)	3.012(6)
Cnt1−Ln(1)−Cnt2	132.6
Cnt3−Ln(2)−Cnt4	132.9
Cnt1−Ln(1)−O(1)	112.7
Cnt2−Ln(1)−O(1)	111.0
Cnt3−Sm(2)−O(2)	109.7
Cnt4−Sm(2)−O(2)	114.1
Cnt1−Ln(1)−C(42)	101.8
Cnt2−Ln(1)−C(42)	106.5
C(43)−C(41)−C(44)	118.6(5)
C(42)−C(41)−C(43)	121.0(5)
C(42)−C(41)−C(44)	120.4(5)

Since the unsolvated alkyl lanthanide complexes, $[(C_5Me_5)_2LnR]_n$, have been shown to display high C−H bond activation reactivity,[1,2,15,24,25,28−31] the metalation chemistry of the TMM complexes was also examined. Addition of toluene to **2** produced a color change from green to brown, and a complex was obtained that had a composition and IR, ^{1}H, and ^{13}C NMR spectra consistent with those of $[(C_5Me_5)_2La(CH_2Ph)]_n$, **9**, eq 11. The Sm TMM complex, **1**, did not react analogously with

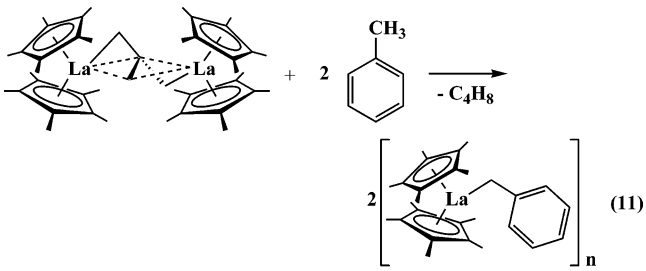

(11)

9

toluene, however. No metalation of benzene or isobutene was observed with any of the TMM complexes.

Discussion

The sequence of reactions involving β-methyl elimination followed by C−H activation that converted the $[(C_5Me_5)_2Sm][(\mu\text{-}Ph)_2BPh_2]/LiCH_2CMe_3$ reaction mixture to the first complex containing both a planar and bridging trimethylenemethane unit, $[(C_5Me_5)_2Sm]_2[\mu\text{-}\eta^3\text{:}\eta^3\text{-}C(CH_2)_3]$, **1**, as shown in Scheme 1 is also applicable to other lanthanides. Specifically, the earlier metals La, Pr, and Nd give analogous products, **2**−**4**. Clearly, the originally isolated **1** is not a special case for Sm, and the cascade of reactions has some generality. The synthesis of **2** provides an opportunity to compare X-ray data with DFT calculations, and the isolation of **3** and **4** allows an evaluation of TMM structure as a function of size and $4f^n$ configuration.

Since the analogous synthetic chemistry did not extend to the smaller metals Y and Lu, there appears to be a size dependence on the reactivity as is often typical in the lanthanide series. The isolation of the neopentyl lutetium complex, $[(C_5Me_5)_2LuCH_2C(CH_3)_3]_x$, **6**, indicates that the first step in the synthetic sequence, the salt metathesis reaction, is still viable with this smallest lanthanide. Moreover, since **6** is observed to β-methyl eliminate to form the methyl complex, $[(C_5Me_5)_2LuMe]_x$, the β-alkyl elimination reaction is also not the factor that precludes TMM formation via Scheme 1. The high C−H bond activation reactivity of $[(C_5Me_5)_2LuMe]_x$ is well-known, but this complex can also insert olefins.[25,29−31] Evidently, among the panoply of reactions available to this reactive species, the formation of the TMM complex is not the favored one under the conditions successful for isolation of **1**−**4**. This appears to be another example of a case in which the factors that control lanthanide reactivity are delicately balanced. The early metals have more steric accessibility, and the reaction proceeds smoothly. Although the smaller metals can engage in the same reactions required to make the TMM product, the more restricted coordination environment generates different results.

A referee has suggested that the metal size dependence of Scheme 1 may result because an intermediate isobutene complex is present. It is possible that with the larger metals, the isobutene formed in the β-Me elimination reaction, the first step in Scheme 1, remains in the coordination sphere of the metal. If this is the case, the next step, the C−H bond activation to form the methyl−allyl complex, would be intramolecular. With the smaller metals, there may not be room for isobutene to coordinate, a situation that would preclude intramolecular formation of the methyl−allyl complex.

The fact that the yttrium TMM complex, $[(C_5Me_5)_2Y]_2[\mu\text{-}\eta^3\text{:}\eta^3\text{-}C(CH_2)_3]$, **5**, can be synthesized from the methylallyl intermediate, $(C_5Me_5)_2Y[CH_2C(Me)CH_2]$, **7**, eq 8, suggests that this is indeed a kinetic problem involving preferred reaction pathways. There is no reason to expect the lutetium TMM complex cannot exist if the proper synthetic route is identified.

The isolation of TMM complexes from the $[(C_5Me_5)_2Ln][(\mu\text{-}Ph)_2BPh_2]/LiCH_2CHMe_2$ reaction sequence shown in Scheme 2 supports the ideas initially proposed for formation of the first TMM complex, **1**, via Scheme 1.[2] The TMM complexes **1**−**5** should be available from a variety of combinations of isobutene and metallocene alkyls and hydrides. The isolation of isobutane rather than hydrogen as a byproduct indicates that the postulated "$[(C_5Me_5)_2Ln(CH_2CHMe_2)$" intermediate is a superior metalation reagent compared to $[(C_5Me_5)_2LnH]_x$. Again a balance of several factors apparently affects the reactivity since this more "atom efficient" route compared to the neopentyl lithium synthesis does not give nearly as good a yield. For $[(C_5Me_5)_2LnR]_n$ and $[(C_5Me_5)_2LnH]_n$ reactions, in general, the specific pathway favored among many options involving β-hydride and β-alkyl eliminations, insertions, and σ bond metatheses will depend in subtle ways on the particular components involved. Fortunately, the steric aspects of this reactivity can be manipulated in the lanthanide series not only by the size of the ligands but also by the size of the metals. In this case, size optimization was critical to obtaining the TMM complexes since they are most readily formed with the larger metals.

The data on the TMM complexes that have been obtained show a similarity between the TMM ligand in all the structures, La−Y, without regard to the metal size. This similarity is also found in the density functional calculations on the two extreme sized metals in the series, La and Lu. All of the structural and theoretical data point to ionic bonding between the TMM ligands

and these metals. In each case, the $[C(CH_2)_3]^{2-}$ ligand has delocalized bonding similar to the calculations obtained on the free ligand. Overall, the $[C(CH_2)_3]^{2-}$ dianion should be a good ligand for the electropositive lanthanide ions. It is a compact six-electron system with two negative charges, an ideal organometallic moiety for bridging two cationic metals.

The DFT studies of this system show both the difficulties and power of this method of analysis. Although DFT calculations of the open shell Sm^{3+} system did not converge, the calculations on the closed shell La^{3+} and Lu^{3+} systems provided structural predictions that matched those obtained experimentally for both the diamagnetic lanthanum and paramagnetic samarium complex. Hence, it may be possible to use the DFT calculations on the two diamagnetic metals with the extremes of size in the lanthanide series, La and Lu, to bracket the expected structural results for the metals in between. Of course, when the lanthanum and lutetium theoretical results differ, this will not be as straightforward.

The fact that the initial calculations on the lanthanum system gave a structure for the TMM ligand that proved to be more accurate than that obtained from the initial crystallographic data shows how useful the DFT method can be in evaluating complexes for which accurate X-ray data are not available. All too often disorder or crystal quality limit the X-ray crystallographic information available on heavy metal complexes. If theoretical calculations can provide more accurate information along with the relevant orbital picture, this extends the amount of information available on these systems.

The initial reactivity studies of the TMM complexes indicate that they appear to access η^1-resonance forms and react like alkyl complexes. In this sense, these bimetallic complexes can be viewed as bifunctional alkyls containing a central vinyl group, as shown in the resonance form in Scheme 3. The reaction of **1** with benzophenone, eq 10, mimics the reactivity of a zirconium TMM complex, eq 9, but does so in a bimetallic fashion such that the C_4 TMM precursor is converted to a C_6 moiety with oxygen and phenyl functionality.

Consistent with the view that the TMM complexes have access to an η^1-alkyl form, some of these complexes participate in C−H bond activation. With the TMM series of complexes, this appears to be highly dependent on metal size. Hence, the lanthanum complex displays this reactivity with toluene, whereas the other complexes of the smaller metals do not. The metalation reactivity is not as high as that for simple alkyls like $[(C_5Me_5)_2LnMe]_n$ in that only toluene and not benzene is metalated by **2**. In contrast the methyl alkyls will metalate benzene and even two of the methyl groups of the $(C_5Me_5)^{1-}$ ligands.[1]

Conclusion

Reaction of the weakly ligated $[(C_5Me_5)_2Ln][(\mu\text{-}Ph)_2BPh_2]$ complexes with neopentyl lithium provides reactive complexes that undergo β-Me elimination and subsequent C−H bond activation reactions to form the planar trimethylenemethane complexes, $[(C_5Me_5)_2Ln]_2[\mu\text{-}\eta^3\text{:}\eta^3\text{-}C(CH_2)_3]$, for La, Pr, and Nd as well as Sm. Although $[(C_5Me_5)_2Ln][(\mu\text{-}Ph)_2BPh_2]$/isobutyllithium reactions would appear to be a more direct route to these C_4 products, the yields of these reactions are lower and the neopentyl route with β-Me elimination is preferred. The overall reaction appears to be metal size dependent since the smaller metals Y and Lu do not react in the same way, although the Y analogue can be accessed by metalation of $(C_5Me_5)_2Y[CH_2C(Me)CH_2]$. DFT calculations on the La and Lu analogues suggest completely delocalized bonding within the trimethylenemethane bridged ligand and largely ionic bonding between the metals and the TMM unit that is consistent with the X-ray crystallographic data. The new TMM complexes react to form symmetrically substituted vinyl complexes as demonstrated by the formation of $[(C_5Me_5)_2Sm]_2[\mu\text{-}(OCPh_2CH_2)_2C{=}CH_2]$ by double insertion of benzophenone into $[(C_5Me_5)_2Sm]_2[\mu\text{-}\eta^3\text{:}\eta^3\text{-}C(CH_2)_3]$.

Acknowledgment. We thank the Chemical Sciences, Geosciences, and Biosciences Division of the Office of Basic Energy Sciences of the Department of Energy for support and the UK EPSRC for computational support through Grant GR/S062333/01.

Supporting Information Available: Synthetic, spectroscopic, and X-ray diffraction details (PDF, CIF). This material is available free of charge via the Internet at http://pubs.acs.org.

JA0645988